East European Journal of Physics. **4.** 118-124 (2022)
DOI:10.26565/2312-4334-2022-4-11 ISSN 2312-4334

EFFECT OF SILVER NANOPARTICLES SILAR CYCLE ON TiO_2 NANOPARTICLES THIN FILM: OPTICAL AND STRUCTURAL STUDY†

Daniel Thomas[a], Eli Danladi[b,*], Mary T. Ekwu[c], Philibus M. Gyuk[a], Muhammed O. Abdulmalik[d], Innocent O. Echi[e]

[a]*Department of Physics, Kaduna State University, Kaduna, Nigeria*
[b]*Department of Physics, Federal University of Health Sciences, Otukpo, Benue State, Nigeria*
[c]*Department of Physics, Airforce Institute of Technology, Kaduna, Nigeria*
[d]*Department of Physics, Confluence University of Science and Technology, Osara, Kogi State, Nigeria*
[e]*Department of Applied Physics, Kaduna Polytechnic, Kaduna, Nigeria*
**Corresponding Author: danladielibako@gmail.com, tel.: +2348063307256*
Received September 20, 2022; revised September 29, 2022; accepted October 7, 2022

Titanium dioxide (TiO_2) has gained a lot of research interests due to its applicability in electronic materials, energy, environment, health & medicine, catalysis etc as a result of its high permittivity, refractive index, efficiency, low-cost chemical inertness, eco-friendliness, photocatalytic activity, photostability and ability of decomposing a wide variety of organic compounds. In this study, the effect of silver nanoparticles (AgNPs) deposited through Successive Ionic Layer Adsorption and Reaction (SILAR) on the optical, structural and morphological properties of TiO_2 was explored systematically. The investigation was achieved via a combined effect of UV-vis spectroscopy, Scanning Electron Microscope (SEM) and X-ray Diffractometer (XRD) characterizing tools. As illustrated from the SEM micrographs, introduction of AgNPs result to enhanced nucleation and films growth with presence of shining surface which can be seen to contribute to good photon management through enhanced light scattering. The XRD results showed that, the presence of AgNPs on TiO_2 results to peaks corresponding to that of the TiO_2 crystallographic planes with no silver peaks detected due to its low concentration in the nanocomposite which shows that it was just homogeneously distributed on the surface of the TiO_2 nanoparticles. The UV-Vis results show a red shift to higher wavelength, showing an increase in visible light absorption which can be ascribed to the strong field effect of the Localized Surface Plasmon Resonance (LSPR). There was a decrease in band gap edge with introduction of AgNPs which indicated an increase in the optical conductivity of the AgNPs modified film.
Keywords: AgNPs, TiO_2, Nanocomposites, LSPR Effect, SILAR
PACS: 61.05.C-, 78.20.-e, 68.37.-d, 81.07.-b, 88.40.H-, 87.64.Ee

1. INTRODUCTION

The wide band gap energy of titanium dioxide prevents it from being active under ultraviolet (UV) light [1-3]. The solar spectrum is composed of 3–5 % UV light and around 40% visible (Vis) light [4]. As such, the photocatalytic properties of TiO_2 observed under sunlight irradiation is less active. There is need for modification of TiO_2 to improve its photocatalytic efficiency under sunlight visible irradiation. Several works have been done to improve TiO_2 so as to render it active in the visible light (400-800 nm) [5-7]. These include: (a) sensitization of TiO_2 with photosensitizers to absorb light in the visible region [8-12], (b) doping TiO_2 with metallic nanoparticles (MNPs) [13,14], and (c) doping TiO_2 with non-metals [15]. Presently, most researchers focus their attention on the MNPs approach by incorporating the metallic nanoparticles to the dense surface of TiO_2 to increase the photoactive wavelength range and enhance the photocatalytic activity under UV irradiation [5-7,13]. Among the doped metals (Ag, Au, Cu, Pt, Nb, Al, B, S, N, Zn, etc), noble metals have attracted significant attentions because of their enhanced properties through Surface Plasmon Resonance (SPR) effect [5,6]. These noble metals serve as scattering centers and sub-wavelength antennas in which the confined electromagnetic energy based on LSPR may greatly improve the absorption factor of the active medium surrounding the NPs [5,13].

Some current reports have shown that metal nanoparticles, such as Ag nanoparticles, augment the catalytic movement in the visible region of the electromagnetic spectrum [16,17]. The results disclosed that the existence of AgNPs is accountable for increasing the photocatalytic activity of TiO_2 in the visible region of sunlight [18].

There are some contradictory results that also reported showing the decreased activity of silver modified titania [12,19]. This may be due to their preparation method, nature of organic molecules, photoreaction medium, or the metal content and its dispersion. Even though there are many studies show the photocatalytic activity of silver doped titania [20-22], the exact mechanism and the role of silver is under debate. In this paper we reported a systematic study of photons initiated photocatalytic activity of screen-printed titania with silver nanoparticles. We discussed the effect on the optical and structural properties and the results show that the introduction of silver nanoparticle in the TiO_2 enhances the optical-response and contributes to the band gap narrowing and also enhances nucleation and grain growth.

† ***Cite as:*** D. Thomas, E. Danladi, M.T. Ekwu, P.M. Gyuk, M.O. Abdulmalik, and I.O. Echi, East Eur. J. Phys. **4**, 118 (2022), https://doi.org/10.26565/2312-4334-2022-4-11

2. MATERIALS AND METHODS

2.1. Preparation of the Cationic Precursor

The AgNPs was prepared by dissolving 0.05 g of silver nitrate in 30 ml of deionized water. Ammonium hydroxide (NH_4OH) was added dropwise. When small amount of NH_4OH was added, Brownish precipitate appears which resulted in silver (I) oxide ($Ag_2O_{(s)}$) formation:

$$2AgNO_{3(aq)} + 2NH_4OH_{(aq)} \rightarrow Ag_2O_{(s)} + 2NH_4NO_{3(aq)} + H_2O_{(l)} \quad (1)$$

When excess NH_4OH was added to silver (I) oxide ($Ag_2O_{(s)}$), colorless solution of diammine silver complex ion was formed:

$$Ag_2O_{(s)} + 4(NH_3 \cdot H_2O)_{(aq)} \rightarrow 2\left[Ag(NH_3)_2\right]OH_{(aq)} + 3H_2O_{(l)} \quad (2)$$

The equation that describes the ionic state of the complex system is given as:

$$\left[Ag(NH_3)_2\right]OH_{(aq)} \Leftrightarrow Ag^+ + OH^- + 2NH_3 \quad (3)$$

2.2. Preparation of the anionic precursor

0.1m (1.13g) Tin (II) chloride was added to 50 ml of distilled water resulting to insoluble $Sn(OH)Cl_{(s)}$:

$$SnCl_{2(s)} + H_2O \Leftrightarrow Sn(OH)Cl_{(s)} + HCl_{(aq)} \quad (4)$$

2 ml of HCl was added in excess:

$$2Sn(OH)Cl_{(s)} + 2HCl_{(aq)} \Leftrightarrow 2SnCl_{2(aq)} + 2H_2O \quad (5)$$

where

$$SnCl_{2(aq)} \rightarrow Sn^{2+} + 2Cl^- \quad (6)$$

2.3. Deposition of TiO_2

The TiO_2 was used as received at its analytical grade level. The TiO_2 was deposited using screen printing technique where a 120 mesh device was used to directly screen print Ti-Nanoxide D/SP on four glass slides. They were dried at 150°C then annealed at 450°C.

2.4. Deposition of AgNPs using SILAR procedure

The glass slide with TiO_2 was immersed in $[Ag(NH_3)_2]^+$ solution for 2 minutes which describes the adsorption process, then rinsed with distilled water for 1 minute to remove excess adsorbed ions from the diffusion layer, and thereafter, it was then transferred to the tin chloride solution for 2 minutes which describes the reduction process. At this point the film turns brownish due to the reduction from Ag+ to Ag, it was then rinsed in distilled water for 1 minute to remove excess unreacted specie. This process is called one (1) SILAR cycle and is as shown in Figure 1 below. The process was repeated for two and three SILAR cycles.

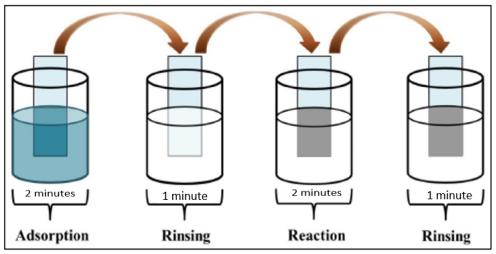

Figure 1. Demonstration of SILAR procedure

2.5. Characterization and Measurement

Optical study of pure TiO_2 and TiO_2 with 1, 2 and 3 SILAR cycles of AgNPs were recorded on Axiom Medicals (UV752 UV-Vis-NIR spectrophotometer). Scanning Electron Microscopy (SEM) images were obtained using Phenom pro-X at an acceleration voltage of 10 kV. Structural analysis of the TiO_2 film was performed using X-ray diffractometer (Rigaku D, Max 2500).

3. RESULTS AND DISCUSSION

3.1. Scanning Electron Microscopy (SEM)

Figure 2a-d show the micrographs of TiO_2 and TiO_2 with 1, 2 and 3 SILAR cycles of silver nanoparticles. The image of the TiO_2 film in Figure 2(a) demonstrates a dense and compact surface which shows a uniformly distributed nanoparticles

with pores for infiltration of introduced materials. As shown from the images (Figure 2b-d), there are presence of shining surfaces which shows a distinct difference with the surface without AgNPs. The presence of the shining particles is an indication of the photocatalytic properties of the introduced AgNPs and also show that it can act as subwavelength antenna to channel incident photons for activation of semiconductor in the visible region for photon management.

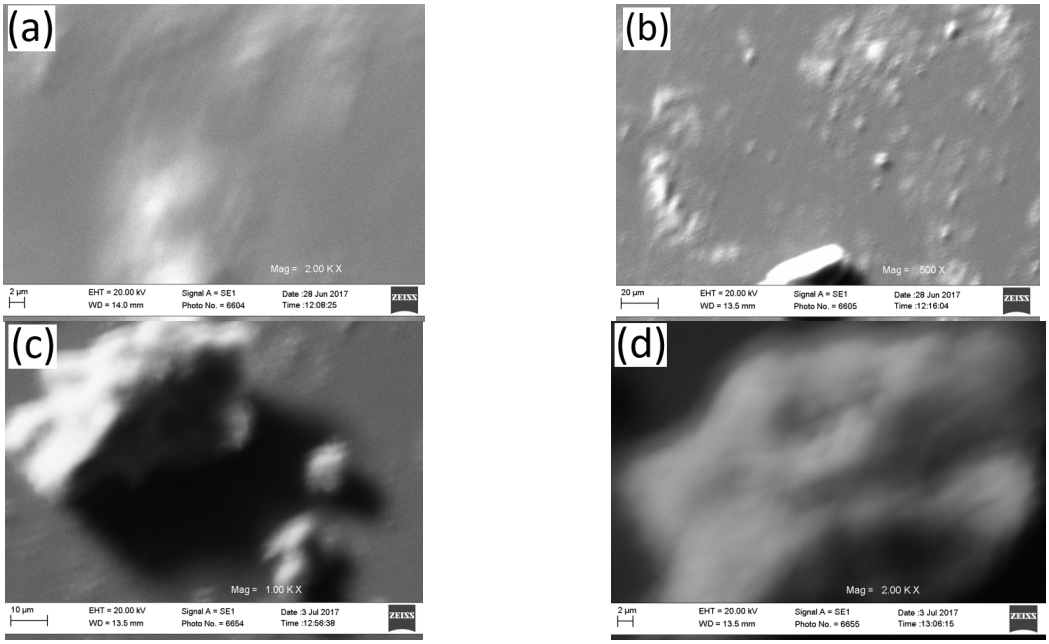

Figure 2. SEM images of: (a) bare TiO_2, (b) TiO_2/1cycle, (c) TiO_2/2cycle, and (d) TiO_2/3cycle at operating voltage of 10 Kv

This AgNPs can broaden the active area of TiO_2 through the introduction of localized surface plasmon resonance (LSPR) effect. When 1 SILAR cycle of AgNPs is introduced, a relatively symmetric distribution of shining particles were observed which can be speculated to contribute to good photon management through enhanced light scattering. The result demonstrates a sample size in the range of 25-55 nm as obtained from Isolution image analyzer with a smooth surface with no aggregated islands. Increasing the number of SILAR cycle from 2 to 3 cycles resulted to formation of significant islands with inhomogeneous distribution of nanoparticles leading to lesser transmittance of light.

3.2. X-ray Diffractometer (XRD)

The XRD pattern of TiO_2, TiO_2 with 1, 2 and 3 SILAR cycles are as shown in Figure 3a-d.

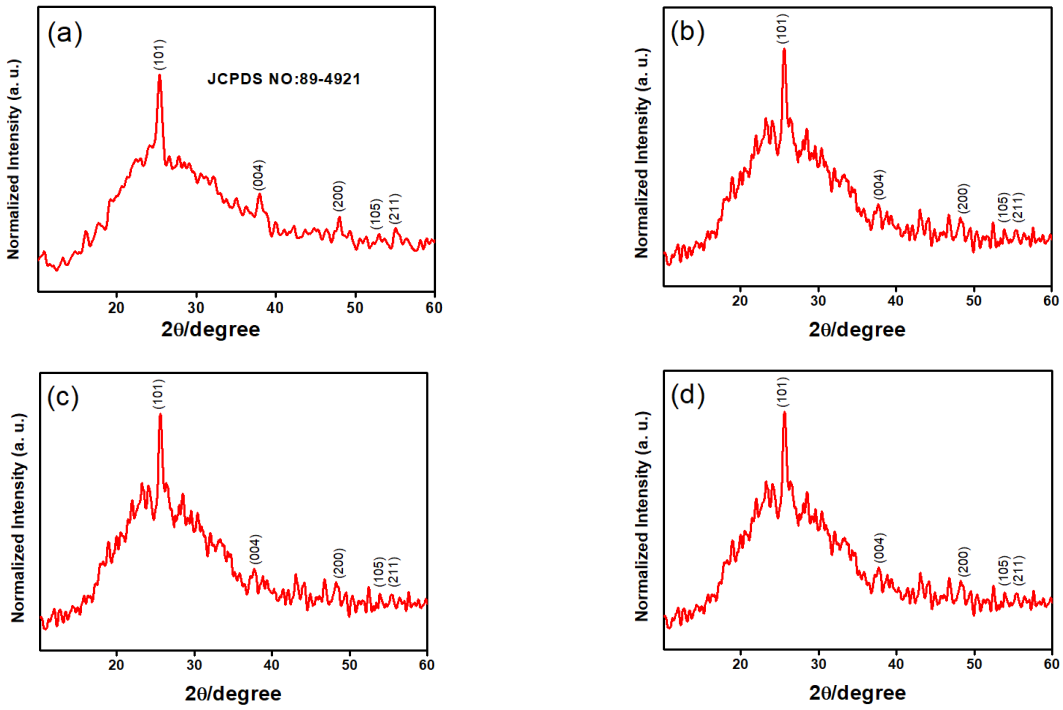

Figure 3. XRD Pattern of: (a) bare TiO_2, (b) TiO_2/1AgNP, (c) TiO_2/2AgNP, and (d) TiO_2/3AgNP

It shows clearly the major peaks at the 2 theta (2θ) angle of 25.36°, 37.87°, 47.97°, 54.93° and 55.45° which corresponds to the planes (101), (004), (200), (105) and (211) respectively. This agrees with the anatase phase of TiO_2 in accordance with JCPDS Card No. 89-4921 with unit cell parameters of 4.9619 Å for TiO_2. This result clearly shows that the TiO_2 nanoparticles were preferentially oriented with (101) face [23]. The anatase phase of TiO_2 is preferred over rutile and brookite for photocatalytic degradation of organic compounds [6,24]. The Fermi level of anatase is ~0.1 eV which is considered higher than that of the rutile phase and as such preferred as a photoelectrode material due to its generation of higher photovoltage over the rutile [25].

After depositing AgNPs on the TiO_2 nanoparticles surface, the observed peaks at the 2 theta angles correspond to that of the TiO_2 crystallographic planes. The peaks due to AgNPs was not detected due to its low concentration which shows that it was just homogeneously distributed on the surface of the TiO_2 nanoparticles [6]. Hence, the peaks are identical for TiO_2 and TiO_2 with 1, 2 and 3 SILAR cycles of AgNPs which shows that TiO_2 was effectively passivated with the AgNPs.

3.3. Optical study

The optical absorbance, transmittance, and reflectance bands of pure TiO_2 and TiO_2 with 1, 2 and 3 SILAR cycles of AgNPs are shown in Figure 4a-c. The measurement was taken at room temperature over the wavelength range of 200-1200 nm.

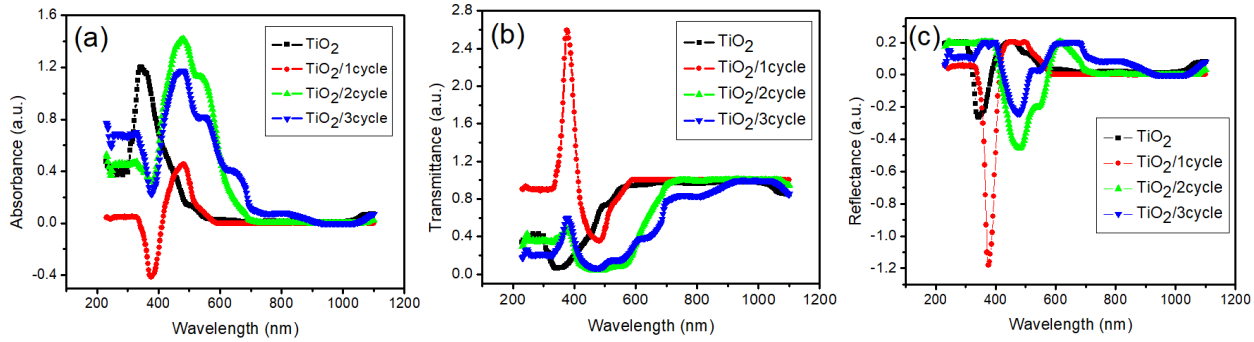

Figure 4 (a) absorbance, (b) transmittance and (c) reflectance against Wavelength

As shown in Figure 4a, the pure TiO_2 can be seen to be absorbing in the UV region with peak around 317 nm which can be attributed to its high refractive index. This property displayed suggests that, modification of the TiO_2 is desirable to make it activated in the visible region. Furthermore, Figure 4a also shows a red-shift towards higher wavelength after introducing AgNPs. This enhanced behavior can be seen to arise significantly through the introduction of LSPR from the deposited AgNPs.

Figure 4(b) presents typical transmittance spectra, which was obtained from the absorbance plot using equation (7).

$$T = 10^{-A} \tag{7}$$

where T is transmittance and A is absorbance.

There was a relatively constant transmittance in the visible to infrared region from 580 nm for TiO_2 and TiO_2 with 1 SILAR cycle of AgNPs. For the 2 SILAR cycle, the constant transmittance was observed from 650 nm. In TiO_2/3cycles nanocomposite, we observed variation in transmittance from the wavelength range of ~739 nm to ~ 1025 nm. It was observed generally, that transmittance intensity was inversely proportional to increase in the AgNPs SILAR cycle. For the reflectance properties, the reflectance was obtained from Equation (8).

$$R = 1 - (A + T) \tag{8}$$

As observed in the micrographs, there was presence of valleys and peaks in the profile with cycle increase. The red shift and the increase in optical path length is attributed to the non-uniform aggregation of the dispersed AgNPs forming the clusters [26] and the effect of interstitial dominance due to introduction of localized defect states during film formation [18].

The refractive index, Extinction coefficient and optical conductivity against photon energy (hv) is as shown in Figure 5a-c.

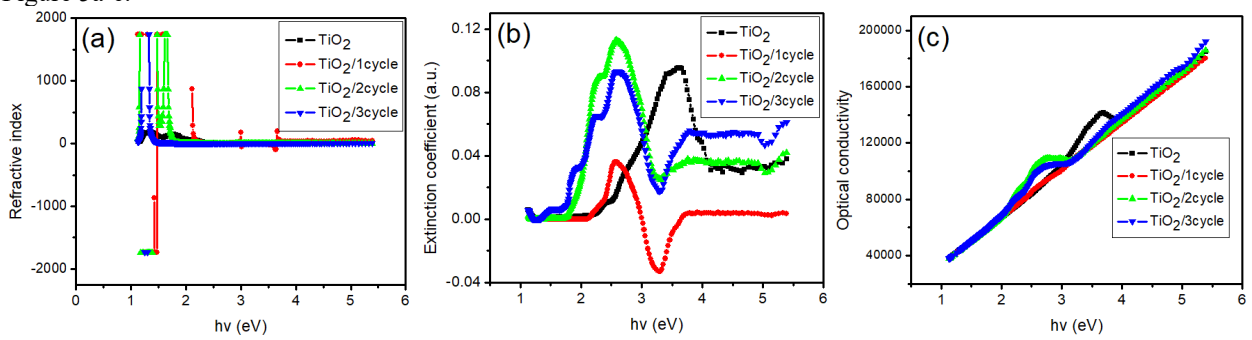

Figure 5. (a) optical refractive index, (b) extinction coefficient, and (c) optical conductivity against photon energy

The refractive index (n) shows the frequencies within a range in which films are not absorbing strongly [27]. The refractive index is crucial in characterizing photonic materials and it was estimated using equation (9), where R is the reflectance.

$$n = \frac{1+\sqrt{R}}{1-\sqrt{R}} \tag{9}$$

$$\alpha = \frac{A}{\lambda} \tag{10}$$

$$k = \frac{\alpha\lambda}{4\pi} \tag{11}$$

$$\sigma = \frac{\alpha nc}{4\pi} \tag{12}$$

The optical behavior of refractive index against photon energy of TiO_2 and TiO_2 with 1, 2 and 3 SILAR cycles of AgNPs is shown in Figure 5a. The results obtained show that the refractive index decreases with the increasing photon energy slightly before maintaining a constant value after 2.3 eV. The observation that the refractive index decreases with increasing photon energy is attributed to the dispersion of light at various interstitial layers present in the composite films.

Figure 5b shows the extinction coefficient versus photon energy as calculated from equation (11), where α is the coefficient of absorption obtained from equation (10) and λ is the wavelength.

The extinction coefficient is referred to the measure of the fractional light loss as a result of scattering and absorption per unit distance of the medium of penetration [27].

It is seen from Figure 5b that the extinction coefficient of all AgNPs modified TiO_2 increases with the increase in the photon energy up to 2.5 eV before it starts decreasing to form a valley at 3.4 eV. This decrease indicates that the fractional loss of light as a result of scattering and absorbance decreases between the range of 2.5 and 3.4 eV. It can also be noted from the figure that the value of extinction coefficient maintains a constant value from ~3.7 to 4.9 eV.

The Optical Conductivity was calculated from equation (12), where σ is the optical conductivity, α is the coefficient of absorption, n is the refractive index and c is the speed of light with magnitude of 3×10^8 m/s.

The variation of optical conductivity with the incident photon energy is shown in Figure 5c. The rise in optical conductivity when the energies of the photon is increasing can be attributed to high absorbance of the films in regions with higher photon energies and also due to increase in absorption coefficient. This can also be seen to arise from increased in density of localized states in the boundaries due to the rise in new defect states [28].

The energy bandgap has been evaluated from the absorption spectra.

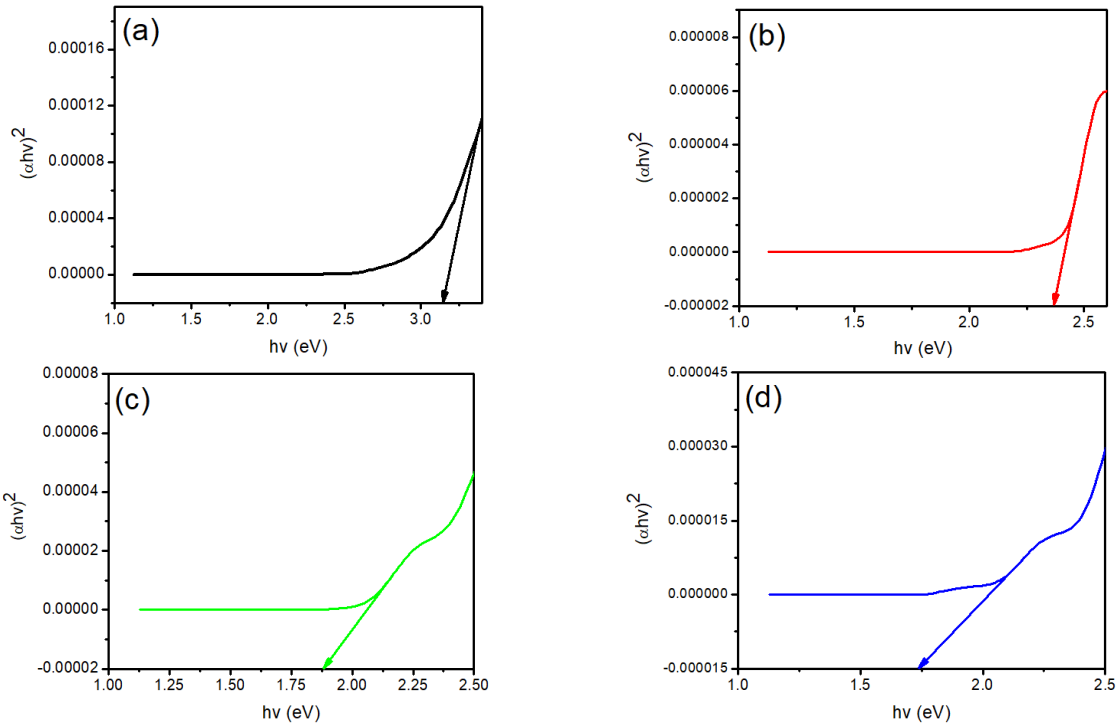

Figure 6. Plot of $(\alpha hv)^2$ against hv for (a) bare TiO_2, (b) TiO_2/1cycle, (c) TiO_2/2cycle, and (d) TiO_2/3cycle

The photocatalytic ability of TiO_2 photocatalyst under visible light is determined by lower bandgap energy (E_g) or absorption in visible light. The energy bandgap (E_g) was determined based on the wavelength of maximum absorption (λ) according to equation (13).

$$E_g = \frac{1240}{\lambda}, \tag{13}$$

here, the maximum absorption wavelength is obtained from the absorption wavelength data.

The E_g was obtained in the formula describes as Tauc plot [29]. The E_g can be obtained from extrapolation of the linear part, $(\alpha hv)^2$ versus hv or $(\alpha hv)^{1/2}$ versus hv plot to $hv = 0$.

Figure 6a-d show the optical band gap of TiO_2 and TiO_2 loaded with 1, 2 and 3 SILAR cycle of AgNPs. As shown from the results, increase in number of SILAR cycles of AgNPs leads to decrease in band gap of the film. A reduction in the band gap demonstrates an increase in the optical conductivity of the material, this is because the electrons will require less energy to cross the fermi energy level of the material [7]. this shows that, a reduction in the band gap energy of the modified samples will yield a better electron transport capability to the conduction band of the pure TiO_2. The band gap of TiO_2, TiO_2/Ag, TiO_2/2Ag, and TiO_2/3Ag nanocomposites are: 3.23 eV, 2.27 eV, 1.88 eV and 1.74 eV.

4. CONCLUSION

The optical, structural and morphological properties of TiO_2 and TiO_2 with 1, 2, and 3 SILAR cycles were investigated using the combined effect of UV-vis spectroscopy, Scanning Electron Microscope and X-ray Diffractometer. The results obtained show that TiO_2 was significantly enhanced to absorb photons at higher wavelength with silver nanoparticles inclusion which is attributed to localized surface plasmon resornance phenomenon from AgNPs. The band gap of TiO_2 was dramatically reduced from 3.23 to 1.74 eV when AgNPs was introduced. The morphological structures of the prepared samples show improved film with uniform distribution of nanoparticles. The structural analyses of the fabricated films show prominent diffraction peaks at 25.36º, 37.87º, 47.97º, 54.93º and 55.45 º which corresponds to the planes (101), (004), (200), (105) and (211) respectively. This agrees with the anatase phase of TiO_2 with unit cell parameters of 4.9619 Å for TiO_2. These results clearly show that silver nanoparticles can enhance optical and structural properties of TiO_2.

Acknowledgement

The authors are grateful to Physics Advanced Laboratory, Sheda Science Technology Complex (SHESTCO) and Namiroch research Laboratory, Abuja for the use of their equipment.

Conflict of interest. Authors have declared that there was no conflict of interest.

Funding. This article did not receive any funding support.

ORCID IDs

Eli Danladi, https://orcid.org/0000-0001-5109-4690; **Muhammed O. Abdulmalik,** https://orcid.org/0000-0002-3250-7864

REFERENCES

[1] M. Pelaez, N.T. Nolan, S.C. Pillai, M.K. Seery, P. Falaras, A.G. Konto, P.S.M. Dunlop, J.W. Hamilton, J.A. Byrne, K. O'shea, M.H. Entezari, and D.D. Dionysiou, Applied Catalysis B: Environmental, **125,** 331 (2012). https://doi.org/10.1016/j.apcatb.2012.05.036

[2] M.K. Seery, R. George, P. Floris, and S.C. Pillai, Journal of Photochemistry and Photobiology: A Chemistry, **189**, 258 (2007). https://doi.org/10.1016/j.jphotochem.2007.02.010

[3] S. Sontakke, C. Mohan, J. Modak, and G. Madras, Chemical Engineering Journal, **189-190**, 101 (2012). https://doi.org/10.1016/j.cej.2012.02.036

[4] M.Y. Onimisi, E. Danladi, T. Jamila, S. Garba, G.J. Ibeh, O.O. Ige, and E. Lucky, Journal of the Nigerian Association of Mathematical Physics, **10**, 177 (2019). http://e.nampjournals.org/product-info.php?pid4037.html

[5] J. Tasiu, E. Danladi, M. T. Ekwu, and L. Endas, Journal of nano and materials science research, **1**, 16 (2022). http://journals.nanotechunn.com/index.php/jnmsr/article/view/1/10

[6] E. Danladi, M. Y. Onimisi, S. Garba, and J. Tasiu, SN Applied Sciences, **2,** 1769 (2020). https://doi.org/10.1007/s42452-020-03597-y

[7] G.A. Alamu, O. Adedokun, I.T. Bello, and Y.K. Sanusi, Chemical Physics Impact, **3**, 100037 (2021). https://doi.org/10.1016/j.chphi.2021.100037

[8] H.M. Chenari, C. Seibelb, D. Hauschild, and H. Abdollahiand, Materials Research, **19**(6), 1319 (2016). https://doi.org/10.1590/1980-5373-MR-2016-0288

[9] K. Nakata, and A. Fujishima, Journal of Photochemistry and Photobiology C: Photochemistry Reviews, **13,** 169 (2012). https://doi.org/10.1016/j.jphotochemrev.2012.06.001

[10] M.R. Hoffmann, S.T. Martin, W. Choi, and W.D. Bahnemann, Chemical Reviews, **95,** 69 (1995). https://doi.org/10.1021/cr00033a004

[11] G. Govindasamy, P. Murugasen, and S. Sagadevan, Materials Research, **19**(2), 413 (2016). https://doi.org/10.1590/1980-5373-MR-2015-0411

[12] T. Daniel, P. M. Gyuk, S. Alhassan, E. Danladi, N. J. Gyuk, P. Anthony, Journal of the Nigerian Association of Mathematical Physics, **54,** 179 (2020). http://e.nampjournals.org/product-info.php?pid4068.html
[13] S. Sreeja, and B. Pesala, Scientific Reports, **10,** 8240 (2020). https://doi.org/10.1038/s41598-020-65236-1
[14] M. Jacob, H. Levanon, and P.V. Kamat, Nano letters, **3,** 353 (2003). https://doi.org/10.1021/nl0340071
[15] J.C. Colmenares, M.A. Aramedia, A. Marinas, J.M. Marinas, and F.J. Ubano, Applied Catalysis A: General, **306,** 120 (2006). https://doi.org/10.1016/j.apcata.2006.03.046
[16] F.L. Yap, P. Thoniyot, S. Krishnan, and S. Krishnamoorthy, ACS Nano, **6**(3), 2056 (2012). https://doi.org/10.1021/nn203661n
[17] G. Kovacs, Z. Pap, C. Cotet, V. Cosoveanu, L. Baia, and V. Danciu, Materials, **8,** 1059 (2015). https://doi.org/10.3390/ma8031059
[18] W.J. Cho, Y. Kim, and J.K. Kim, ACS Nano **6,** 249 (2012). https://doi.org/10.1021/nn2035236
[19] V. Vamathevan, R. Amal, D. Beydoun, G. Low, and S. McEvoy, Journal of Photochemistry and Photobiology A: **148**, 303 (2002). https://doi.org/10.1016/j.cej.2003.05.004
[20] M. Sökmen, D.W. Allen, F. Akkaş, N. Kartal, and F. Acar, Water, Air, and Soil Pollution, **132,** 153 (2001). https://doi.org/10.1023/A:1012069009633
[21] H.M. Sung-Suh, J.R. Choi, H.J. Hah, S.M. Koo, and Y.C. Bae, Journal of Photochemistry and Photobiology A, **163**, 37-44 (2004). https://doi.org/10.1016/S1010-6030(03)00428-3
[22] L. Zhang, J.C. Yu, H.Y. Yip, Q. Li, K.W. Kwong, A. Xu, and P.K. Wong, Langmuir, **19**, 10372 (2003). https://doi.org/10.1021/la035330m
[23] S. Kalaiarasi, and M. Jose, Applied Physics A, **123**, 512 (2017). https://doi.org/10.1007/s00339-017-1121-0
[24] M. Sahu, B. Wu, L. Zhu, C. Jacobson, W.N. Wang, N. Jones, Y. Goyal, Y.J. Tang, and P. Biswas, Nanotechnology, **22**, 415704 (2012). https://doi.org/10.1088/0957-4484/22/41/415704
[25] K.M. Mansoob, A. Sajid, M. Ansari, A. Ikhlasul, L. Jintae, and H.C. Moo, Nanoscale, **5,** 4427 (2013). https://doi.org/10.1039/C3NR00613A
[26] C. Chambers, S.B. Stewart, B. Su, H.F. Jenkinson, J.R. Sandy, and A.J. Ireland, Dental Materials, **33,** e115–e123 (2017). https://doi.org/10.1016/j.dental.2016.11.008
[27] I.L. Ikhioya, E. Danladi, O.D. Nnanyere, and A.O. Salawu, Journal of the Nigerian Society of Physical Sciences, **4**(1), 123 (2022). https://doi.org/10.46481/jnsps.2022.502
[28] N.F. Mott, and E.A. Davis, *Electronic processes in non-crystalline materials*, 2nd edition, (Clarendon, Oxford, 1979).
[29] J. Tauc, editor, *Amorphous and Liquid Semiconductors*, vol.159, (Plenum Press, NewYork, 1974).

ВПЛИВ СИЛЯРНОГО ЦИКЛУ НАНОЧАСТИНОК СРІБЛА НА ТОНКУ ПЛІВКУ НАНОЧАСТИНОК TiO_2: ОПТИЧНЕ ТА СТРУКТУРНЕ ДОСЛІДЖЕННЯ

Деніел Томас[a], Елі Данладі[b], Мері Т. Екву[c], Філібус М. Гюк[a], Мухаммед О. Абдулмалік[d], Інокентій О. Ечі[c]
[a]Фізичний факультет Державного університету Кадуна, Кадуна, Нігерія
[b]Фізичний факультет Федерального університету наук про здоров'я, Отукпо, штат Бенуе, Нігерія
[c]Фізичний факультет, Технологічний інститут ВПС, Кадуна, Нігерія
[d]Фізичний факультет, Об'єднаний університет науки і технологій, Осара, штат Когі, Нігерія
[e]Факультет прикладної фізики, Кадуна Політехніка, Кадуна, Нігерія

Діоксид титану (TiO_2) викликав значний дослідницький інтерес через його застосування в електронних матеріалах, енергетиці, навколишньому середовищі, здоров'ї та медицині, каталізі, що є результатом його високої діелектричної проникності, показника заломлення, ефективності, низької вартості хімічної інертності, екологічності, фотокаталітичної активності, фотостабільності і здатності розкладати широкий спектр органічних сполук. У цьому дослідженні було систематично досліджено вплив наночастинок срібла (AgNP), нанесених шляхом послідовної адсорбції та реакції (SILAR), на оптичні, структурні та морфологічні властивості TiO_2. Дослідження було досягнуто за допомогою комбінованого ефекту ультрафіолетової спектроскопії, скануючої електронної мікроскопії (SEM) і рентгенівської дифрактомії (XRD). Як видно з мікрофотографій SEM, введення AgNPs призводить до посиленого зародження та росту плівок із наявністю блискучої поверхні, яка, як можна побачити, сприяє хорошому управлінню фотонами через посилене розсіювання світла. Результати XRD показали, що наявність AgNPs на TiO_2 призводить до піків, що відповідають пікам кристалографічних площин TiO_2, без піків срібла через низьку концентрацію срібла в нанокомпозиті, що показує, що він просто рівномірно розподілений на поверхні наночастинок TiO_2. Результати UV-Vis показують червоний зсув у бік вищої довжини хвилі, показуючи збільшення поглинання видимого світла, яке можна віднести до сильного ефекту ближнього поля та ефекту дальнього поля локалізованого поверхневого плазмонного резонансу (LSPR). Спостерігалося зменшення краю забороненої зони із введенням AgNP, що вказує на збільшення оптичної провідності плівки, модифікованої AgNP.

Ключові слова: AgNPs, TiO_2, нанокомпозити, LSPR ефект, SILAR